Chapter 5

Preliminary Experiments at Tokamaks

In order to assess whether the beam emission profiles of visible HeI lines can serve for a diagnostic for n_e- and T_e profiles, experiments have been performed by Mr. M. Proschek and Dr. H.-D. Falter of this institute at the ASDEX Upgrade ('AUG') tokamak in Germany and the JET tokamak in the UK. For these experiments the existing neutral-beam heating systems were applied to produce fast neutral He-atom beams of a few hundred milliseconds duration. For the measurement of the beam-emission profile, spectrometers dedicated to ion-temperature measurements have been used. The aim of these experiments was to

- verify which He lines have sufficient intensity to be used, to
- measure beam-emission profiles, and to
- compare them with the corresponding profiles calculated with our code.

Ideally, one should use repetitive discharges with no or only little variations in the density- and temperature profiles for the various He emission lines. Furthermore, the discharge should be in steady state during the He-beam injection, thus allowing sufficiently long integration times to identify variations in the beam emission caused by the He injection.

The first experimental attempt to assess the suitability of a fast He beam for beam-emission diagnostics have been made at ASDEX Upgrade. One of the 4 beam sources of one neutral-beam injector was converted from hydrogen to He producing a 30 keV beam with an equivalent neutral-beam current of about 14 A. Helium was injected during some ten discharges. For the experiments at JET, so-called 'doped' beams were produced, i.e. neutral deuterium beams with a small fraction of He atoms. In the next subsections the sequence of these

experiments is described and the most important results are discussed. A more detailed description has already been given in [90].

5.1 Experiments at ASDEX Upgrade

The experiments performed at ASDEX Upgrade ('AUG') in late July and early August 1999 were our first experimental attempt to assess the suitability of a fast He beam as beam-emission diagnostics. For these experiments pure He-atom beams were produced by running one of the neutral beam sources with He instead of deuterium or hydrogen. This was easy to realize as no hardware modifications were required. The drawback of this method is that the beam source used will not be available for plasma heating. Also, He gas accumulates in the neutral-injector box, since it is not pumped by the titanium getter pumps. The rise in partial pressure in the injector box leads to increased losses due to charge-changing collisions and limits the pulse duration of the injector. Hence, the duration of the He beam injection was set to 300 ms or less and He injection could only be performed at the end of a discharge.

AUG has two beam injectors with four beam sources each. The He injection was carried out with source 4 of the so-called 'SO' ('süd ost' in german) injector rated for 60 keV beam energy and 78 A ion-beam current in deuterium per beam source. The source was operated at half the extraction voltage of the other sources of that injector, namely 30 keV and 27 keV, respectively. The so produced neutral He beams had an equivalent injected neutral-beam current of about 14 A.

For the spectroscopic measurements the standard horizontal charge-exchange spectroscopy system ('CER') with 16 lines of sight could be used for plasma discharges in which the measurement of the ion temperature was not required. This condition severely limited the number of discharges available for measurements of the He-beam emission. To overcome this limitation 3 spare fibres from the CER diagnostic which viewed the plasma near the plasma center where routed to a second spectrometer from the Li-beam diagnostic. Initially this spectrometer was used to identify the most intense He lines. However, it turned out that the intensity of the Doppler-shifted He line was weak, and in order to distinguish this line from other unshifted peaks at this wavelength one has to verify that the Doppler shift varies with the viewing angle. Later on, it was also discovered that the preamplifier of this spectrometer was faulty. As a consequence only the measurements with the CER spectrometer were suitable for evaluation. The measured spectra are usually analysed by a fitting routine using

a Gaussian distribution to fit the Doppler-shifted intensity after applying a linear background subtraction. The error bars in the figures showing the experimental results (figures 5.4 to 5.7) represent the quality of these fits.

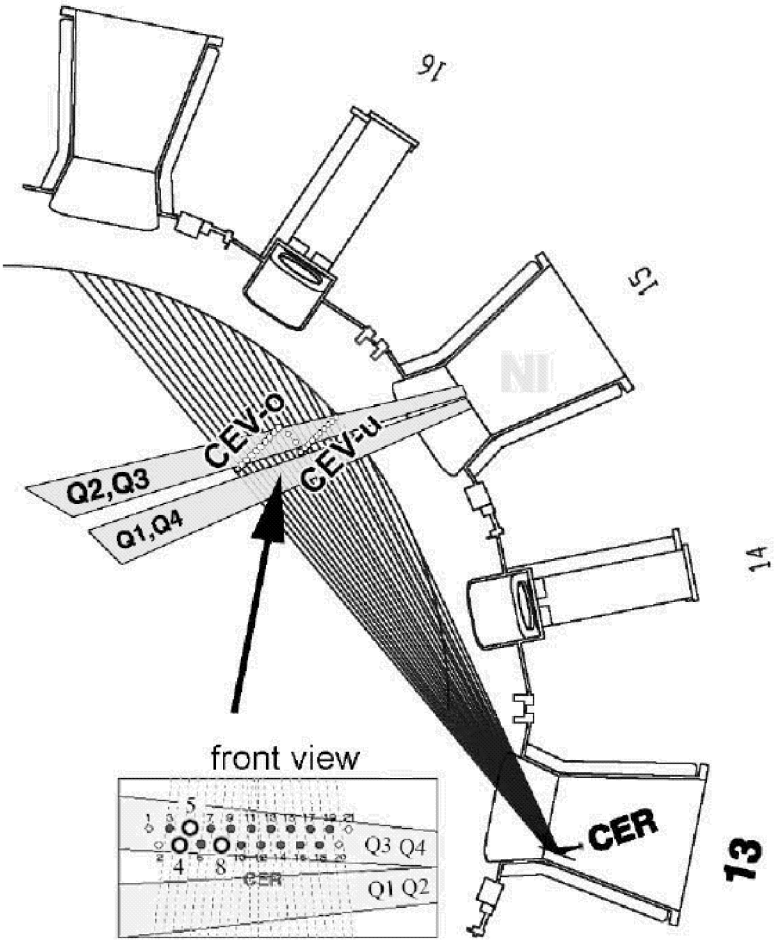

Figure 5.1: Top view of the schematics of the CER diagnostic system at ASDEX Upgrade. The black lines denote the lines of sight, the grey bars denote the four heating-beam paths (Q_1 to Q_4). The position of the lines of sight vs. beam path is also shown in front view. The fibres for the CER diagnostic are marked by dots, those for the Li-beam diagnostics are marked by open circles.

The geometry of the CER spectroscopic system is shown in figure 5.1. The fibres of the CER diagnostic view the plasma from the edge to the plasma center. The angles between the lines of sight used for the experiments and the beam are given in table 5.1. Near the scrape-off layer the viewing angle is close to 90°. Hence, the Doppler shift for the fibres viewing the plasma edge (#18 and #19) is too small to be resolved satisfactory, consequently these data points have been left out of the analysis.

line of sight	major radius	viewing angle
#3	1.67 m	74.6°
#6	1.77 m	77.0°
#7	1.80 m	77.6°
#9	1.86 m	79.1°
#10	1.89 m	79.9°
#11	1.92 m	80.6°
#12	1.96 m	81.5°
#13	1.98 m	82.1°
#14	2.02 m	83.0°
#15	2.05 m	83.6°
#16	2.08 m	84.4°
#17	2.11 m	85.1°
#18	2.14 m	85.9°
#19	2.17 m	86.6°

Table 5.1: Viewing angle between the lines of sight and the He beam and major radius of the beam segment viewed by the fibres of the CER diagnostic system used for the first experiments at ASDEX Upgrade.

The intensity of the Doppler-shifted peaks is about by one order of magnitude lower than that of the corresponding unshifted peaks of all observed wavelengths for all lines of sight. The unshifted He emission originates from He gas in the plasma edge as thermalized He atoms can not penetrate deeper into the plasma. The majority of these He atoms in the plasma edge do not originate from the He beam, as the unshifted emission starts well before He gas is released into the injector. One possible source for this He is the first wall, which is subjected to He glow-discharge cleaning between most of the discharges.

The experiments provided three discharges in which the He-beam emission spectra could be evaluated, namely #12635 with 502 nm, #12643 with 588 nm, and #12644 with 668 nm. All three discharges have been performed with hydrogen plasmas. The last two discharges where almost identical ohmic plasmas with some ECR heating at 3 s and He injection at 4.2 s - 4.5 s after plasma initiation. During discharge #12635 the plasma was mainly heated by neutral-beam injection. The He beam was injected at 4.8 s - 5.1 s after plasma initiation. The T_e- and n_e profiles used for the model calculations (figures 5.2 and 5.3) are taken from Thomson scattering measurements. Table 5.2 shows the He-beam parameters used for calculation of the line-emission profiles for the three presented discharges.

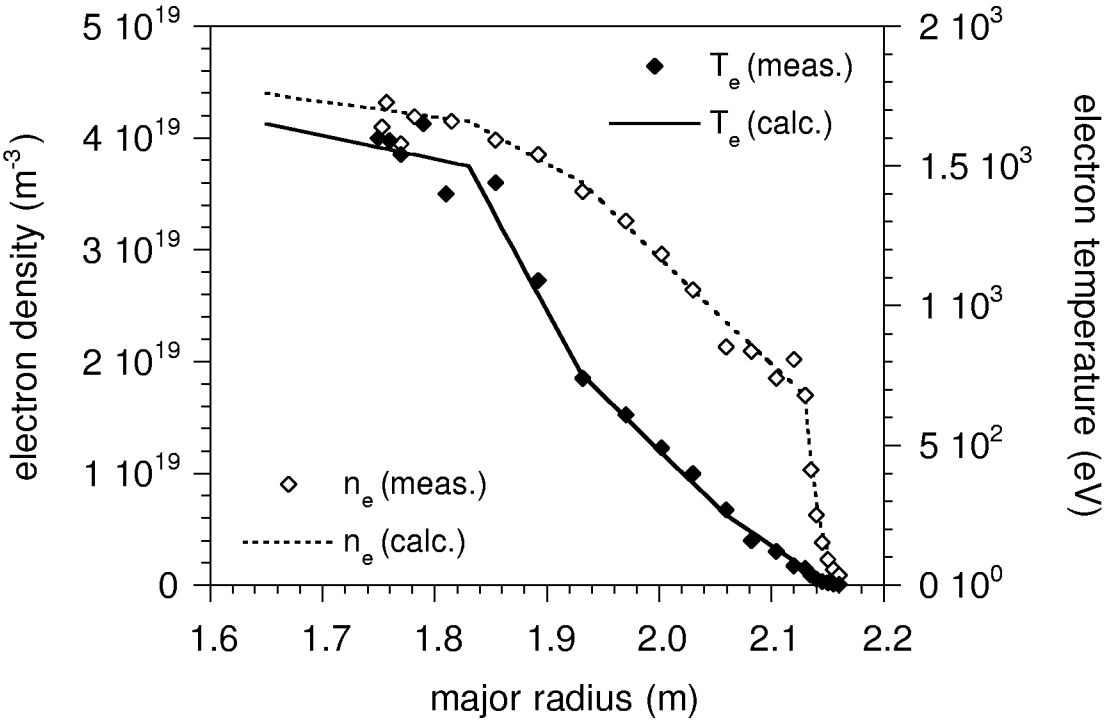

Figure 5.2: T_e and n_e profiles of AUG discharge #12643: Thomson scattering results (diamonds) and therefrom derived profiles used for model calculations (lines).

discharge number	equivalent beam current	beam energy	measured wavelength	corresponding transition
12635	14.2 A	27 keV	502 nm	$3^1P \rightarrow 2^1S$
12643	14.2 A	27 keV	588 nm	$3^3D \rightarrow 2^3P$
12644	14.2 A	27 keV	668 nm	$3^1D \rightarrow 2^1P$

Table 5.2: Discharge number, beam parameters and observed wavelength of the three evaluable measurements at ASDEX Upgrade.

The He beam is inclined by 10.84° in the horizontal plane and 4.9° in the vertical plane, and the beam-path increment is therefore not equal to that of the major radius. The model calculations are performed following the beam-interaction length L_{bi}. n_e- and T_e profiles are being mapped onto L_{bi}. The axis of the AUG vacuum vessel is located at $R_{maj} = 1.65$ m for the presented experiments, the outer separatrix at $R_{maj} = 2.11$ m for #12635 and at $R_{maj} = 2.13$ m for #12643 and #12644.

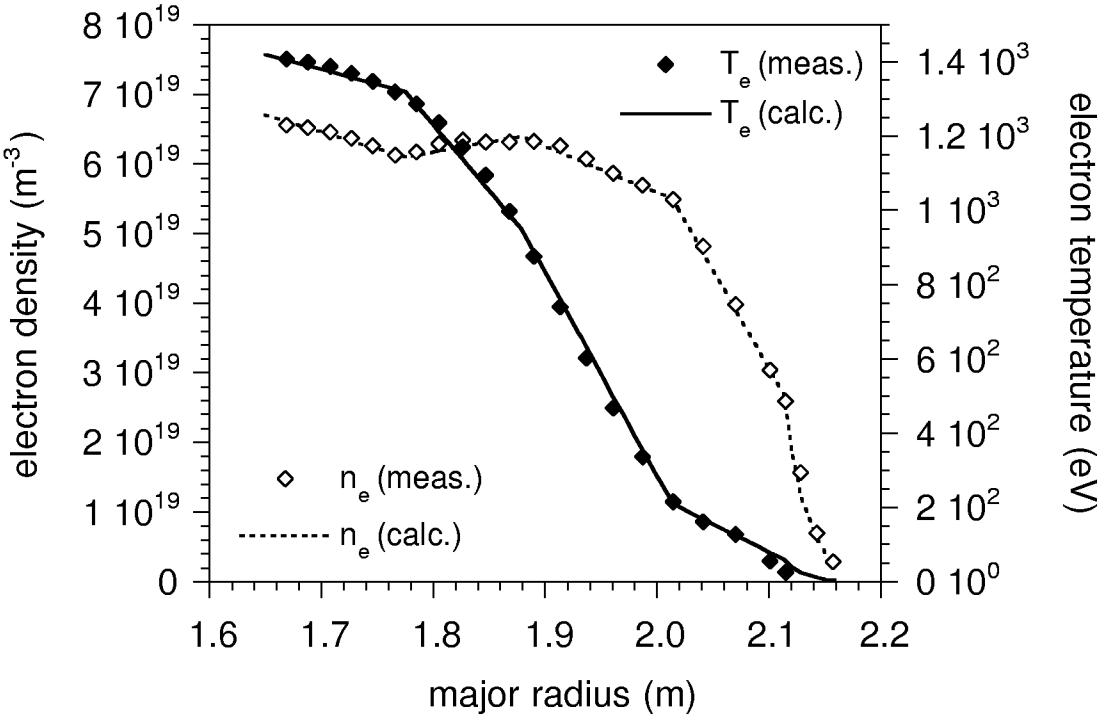

Figure 5.3: T_e and n_e profiles of AUG discharge #12635: Thomson scattering results (diamonds) and therefrom derived profiles used for model calculations (lines).

The minimum distance between the beam axis and the various lines of sight are staggered and slightly offset against each other, see figure 5.1 (front view). This means that the beam intensity is different, depending on this distance. The exact width of the AUG He beam is not known. In this paper we assume a Gaussian profile with a divergence of 0.9° which corresponds to a fall-off length of 120 mm. Moving from the plasma center to the edge, the distance between beam axis and the lines of sight increases. The measured beam emission signal I_ν from line of sight ν has therefore to be corrected by a factor f,

$$f = e^{\frac{\Delta^2}{\lambda^2}}, \tag{5.1}$$

where Δ gives the offset between beam axis and lines of sight and λ the fall-off length of the beam. The correction is small for $\Delta \ll \lambda$. If Δ becomes comparable to λ, as in the case for the outer lines of sight, the correction becomes significant and is critically dependent on the exact knowledge of the beam alignment and the beam profile. As an illustration of the sensitivity of the correction factor to the alignment of the beam, table 5.3 shows f for several examples of beam divergence for one line of sight with the smallest distance to the beam axis (#6) and for one line of sight with a large distance to the beam axis (#17).

It can be seen that the correction for lines of sight in the plasma center are not much affected by uncertainties in the beam divergence, whereas the correction for lines of sight near the plasma edge is very sensitive to such changes. In addition to this effect also the uncertainty in the beam alignment leads to a much bigger error for the lines of sight near the plasma edge than for the ones in the plasma center.

line of sight	Δ in mm	f (0.9°)	f (1.1°)	f (0.7°)
#6	15	1.016	1.011	1.027
#17	97	2.030	1.606	3.223

Table 5.3: Distance between beam axis and lines of sight (Δ) and correction factor f for three different values of the beam divergence for the line of sight with the smallest Δ (#6) and with a large Δ (#17).

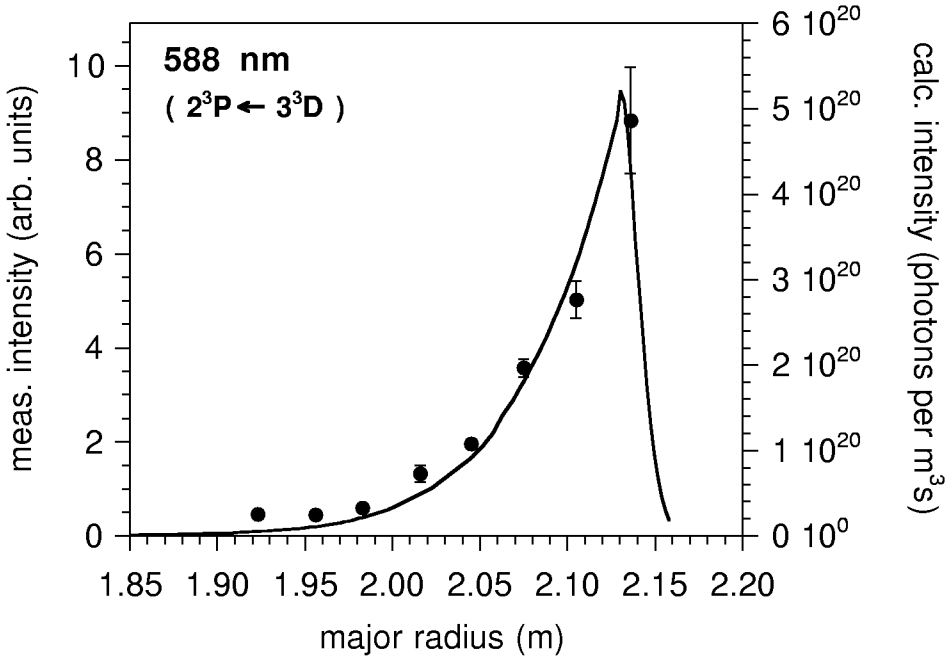

Figure 5.4: Comparison of measured (black circles) and calculated (solid line, based on T_e- and n_e profiles shown in figure 5.2, assuming 2% 2^3S fraction) line emission at 588 nm for AUG discharge #12643.

Figures 5.4 and 5.5 show comparisons of measured and calculated line intensity profiles for discharges #12643 and #12644 assuming an initial 2^3S fraction of 2%.

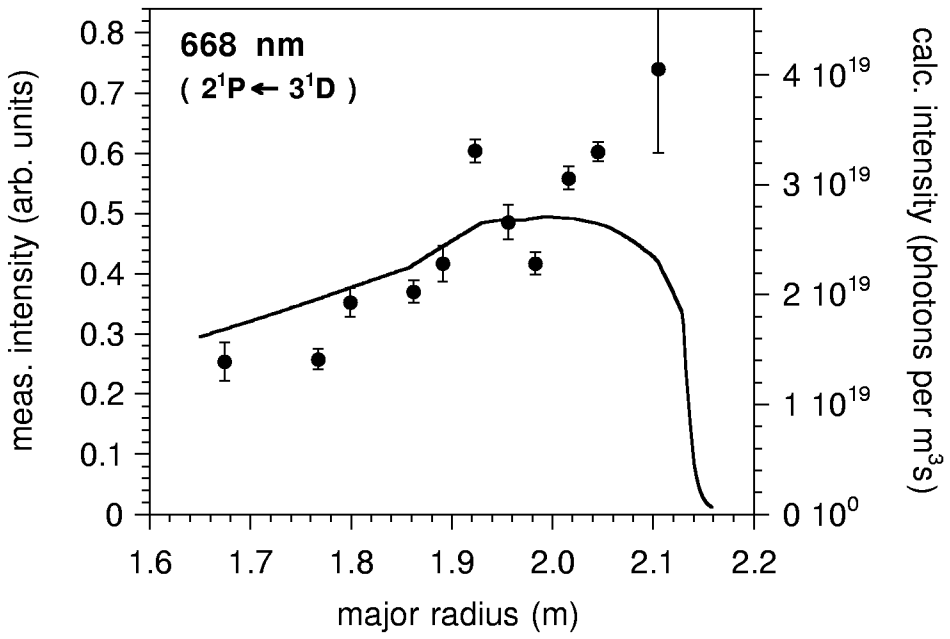

Figure 5.5: Comparison of measured (black circles) and calculated (solid line, based on T_e- and n_e profiles shown in figure 5.2, assuming 2% 2^3S fraction) line emission at 668 nm for AUG discharge #12644.

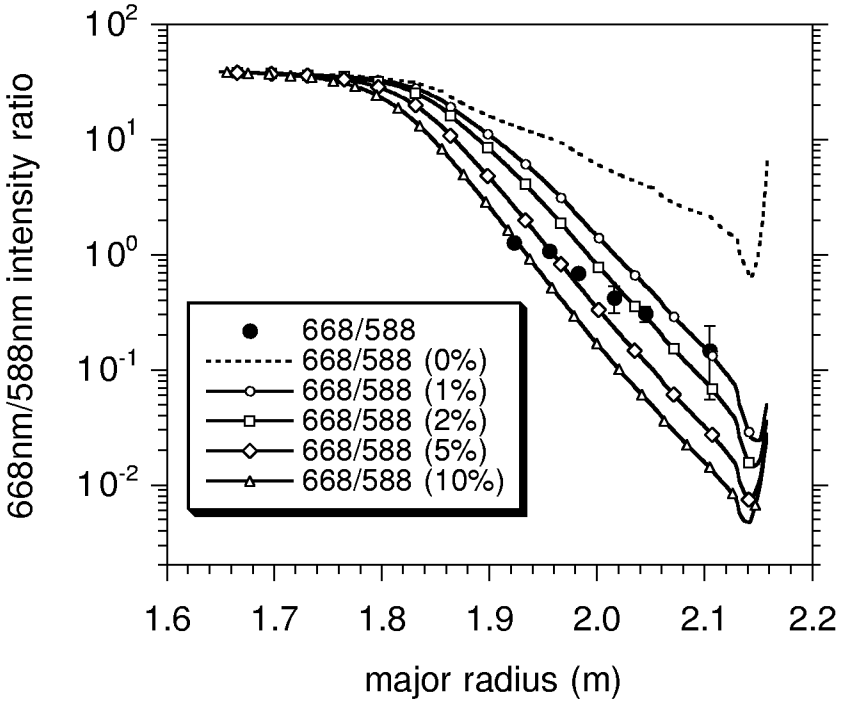

Figure 5.6: Comparison of measured (black circles) and calculated (solid lines, based on plasma profiles shown in figure 5.2, assuming 0%, 1%, 2%, 5%, and 10% initial 2^3S fraction) 668 nm/588 nm line-intensity ratio for AUG discharges #12644 and #12643, respectively.

As already mentioned, the error bars displayed in the figures are a measure for the quality of the fit of the Doppler-shifted peaks only. The large error bar for the outermost point can be explained by the insufficient separation between shifted and unshifted peak. An additional error for the outermost points is possible because of their sensitivity to beam alignment and beam profile, as described above. The observed emission lines are well represented by the model calculations.

As the line-intensity ratios between emission lines of different spin systems is rather sensitive to the initial metastable fraction, the measured 668 nm/588 nm line-intensity ratio has been compared to the corresponding calculated ones for several initial metastable fractions, see figure 5.6. Once again, an initial 2^3S fraction of about 2% seems to be appropriate.

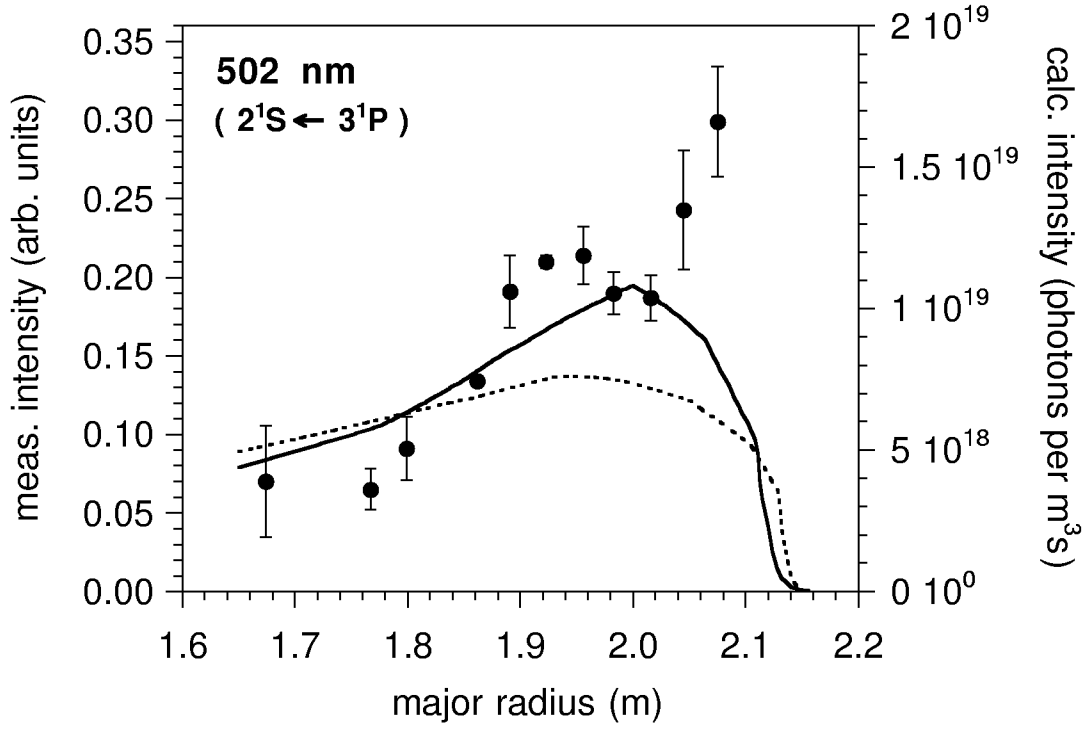

Figure 5.7: Comparison of measured (black circles) and calculated (solid line, based on T_e- and n_e profiles shown in figure 5.3, assuming 2% 2^3S fraction) line emission at 502 nm for AUG discharge #12635. In addition, the calculated 502 nm emission based on the n_e- and T_e profiles of discharge #12643 shown in figure 5.2 (broken line) is displayed.

Figure 5.7 shows a comparison of measured and calculated line intensities at 502 nm for discharge #12635 (based on T_e- and n_e profiles shown in figure 5.3). To illustrate the sensitivity of the calculated emission profile to the input parameters (n_e- and T_e profiles), we show a second 502 nm-emission profile in the calculated profile in figure 5.7.

For this second profile we used the data from discharge #12643 (cf. figure 5.2) instead of that from discharge #12635 (cf. figure 5.3) as input parameters for the modelling. This results in an obvious mismatch between measured and calculated profile. The observed emission line is well represented by the calculation using the correct input files.

5.2 Experiments at JET

The tokamak JET (Joint European Torus) is according to its plasma volume by one order of magnitude larger than AUG, but has about the same heating power in the neutral injection system. Because of this clear lack in heating power the loss of beam power caused by conversion of a beam source to He gas was not acceptable. This led us to the concept of a so-called 'doped' beam, where He gas is temporarily injected additionally to H into a heating-beam source. This was achieved by modifying the gas-inlet system of one of the heating-beam sources. The addition of a He minority (about 10%) does not cause a measurable reduction in heating power which was a prerequisite for carrying out He-injection experiments at JET. These experiments have taken place in mid October and at the beginning of December 1999.

Like AUG, JET has two heating-beam injection systems, one in octant 4 and the other one in octant 8. For our experiments we used PINI 6 of the injector in octant 4 which is rated for 80 keV deuterium beams with 50 - 55 A extracted beam current. By injecting a small flux of He into the ion source operating with deuterium, a He beam with an energy of 75 keV and about 4 A equivalent current was produced. The addition of He had no measurable effect on the beam quality and the transmitted power in the beam-injection system [90]. The He injection has no measurable influence on the impurity level of the plasma as the time trace of Z_{eff} shows no change during He injection. Hence, the doped beam was used at JET on a routine basis. The heating beam was doped with He for 0.5 s at the beginning of the so-called 'flat-top phase' of the discharge, i.e. the phase in which all major plasma parameters (T_e, n_e, heating power, toroidal field, plasma current, etc.) are about constant.

The emission of the He beam was measured with the so-called 'KS7' [93] normally dedicated to ion-temperature measurements. The lines of sight of KS7 are aligned to the beam of PINI 4, but they also cross the beam of PINI 6. The spectrometer on KS7 is optimized for the CVI ($n = 8 \rightarrow 7$) transition at 5291 Å. KS7 uses two spectrometers in series with the first spectrometer acting as a narrow bandwidth filter. If used at wavelengths away from 5291 Å the spectrometer has only its full sensitivity for a narrow band with a considerable reduction

in sensitivity to either side. Attempts have been made to correct this by multiplying the measured signal with a factor compensating the loss in sensitivity. This factor has been obtained by calibrating the spectrometer. So far this procedure is not satisfying and leads to a large scatter in the measured data.

The geometry of the spectroscopic system - consisting of lines of sight viewing top-down ('upper chords') and lines of sight viewing bottom-up ('lower chords') - is shown in figure 5.8.

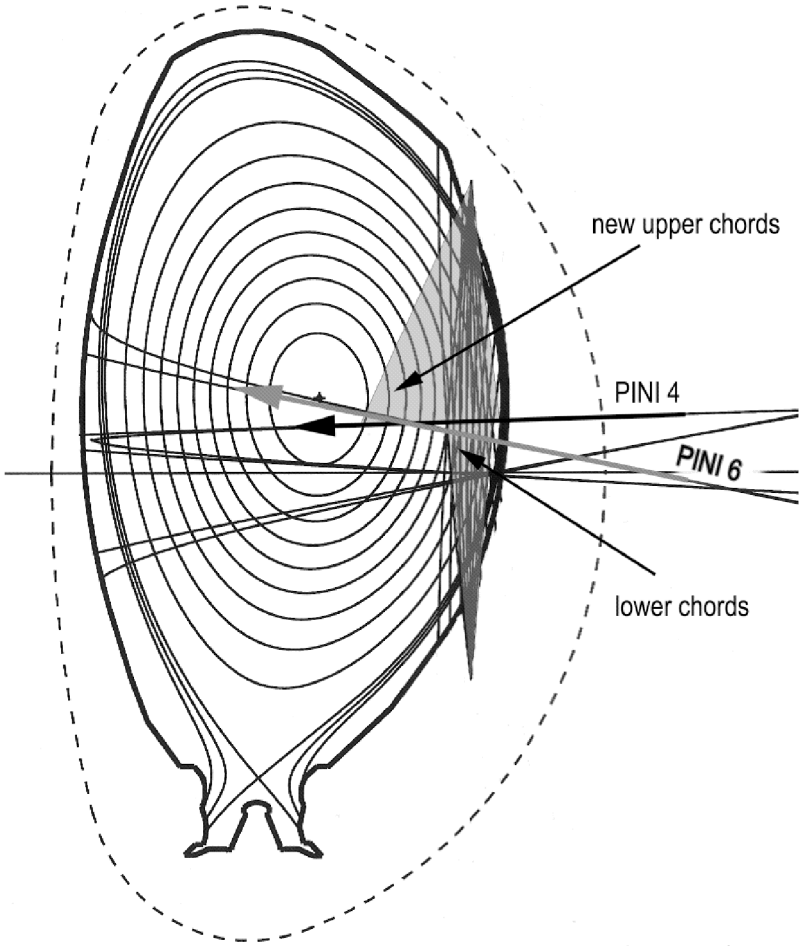

Figure 5.8: Geometry of the spectroscopic system used during the experiments at JET. The grey triangles denote the lines of sight, and the line inscribed with 'PINI 6' denotes the He-beam path.

The upper chords, installed during the 1999 shutdown, cover a larger range of the beam path (major radius R_{maj} 3.19 to 3.90 m). These lines of sight have not yet been end-to-end calibrated and only cross-calibrated with the calibrated lower chords. The width of one line of sight at the location of the beam path is about 10 mm for the lower and 50 mm for the

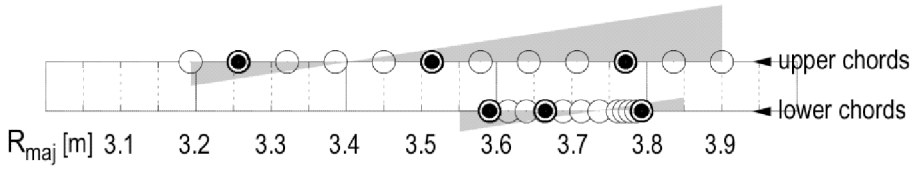

Figure 5.9: Positions of the intersections of the lower and upper chords of KS7 with the beam path of PINI 6 at JET. The grey triangles denote the Doppler shift of the lines of sight.

upper chords. The Doppler shift is zero for the upper chords at $R_{maj} = 3.4$ m and for the lower chords at $R_{maj} = 3.75$ m, which is illustrated in figure 5.9, because at these positions the angle between the lines of sight and the beam is 90°. For some fibres near these positions it was not possible to separate the Doppler-shifted- from the unshifted emission.

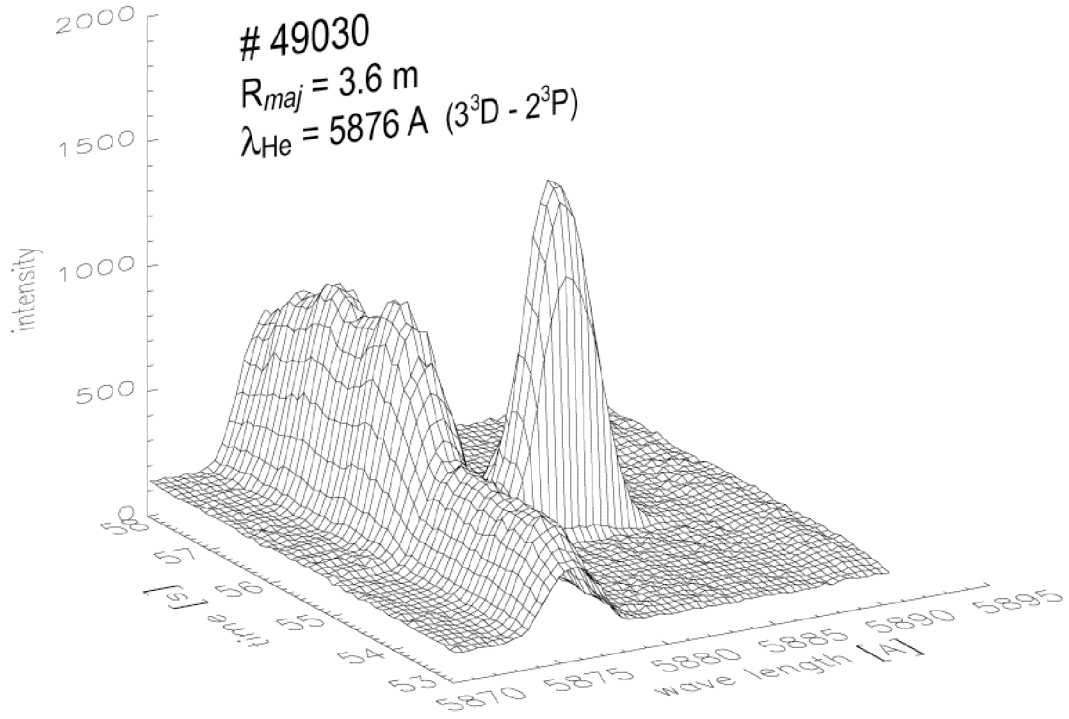

Figure 5.10: Measured intensity spectrum for discharge #49030 in the wavelength region 5870 Å to 5895 Å.

The recorded spectra contain an unshifted intensity and a Doppler-shifted intensity as shown in figure 5.10. As already mentioned in chapter 5.1, the unshifted intensity originates from He atoms in the plasma excited by collisions with other plasma particles. The penetration depth of neutral He is essentially limited to the scrape-off layer where the unshifted intensity must therefore come from. Hence, the intensity of the unshifted radiation is proportional to the gas density in the scrape-off layer. A possible correlation of the unshifted peak with the heating beam can only exist via the energy dependence of the excitation cross sections. The Doppler-shifted intensity originates from fast He atoms in the beam. This intensity is therefore correlated to the timing of the He-beam injection.

The measured data was analyzed in two different ways. If possible, Gauss functions are fitted to both shifted- and unshifted peak, using a suitable subtraction of the background intensity. The intensity of the He beam emission is then calculated from the respective fit parameters. If the Doppler shift becomes so small that the two peaks cannot be resolved, this procedure fails and the second method - the time-trace method - is used. The measured intensity trace of the wavelength-integrated signal consists of Doppler-shifted- and background intensity (including the unshifted peak). Before He injection the intensity is essentially constant, rises during He injection and settles to a new equilibrium value after He injection, see figure 5.10. Before and after He injection all the intensity must originate from the background radiation. It is assumed that this radiation changes its intensity during He injection as the He-background pressure changes. The time constant of that change is assumed to be the same as the time constant of the pressure change in the injector. With this assumption the progression of the background signal during He injection can be obtained. The beam emission signal is the difference between background signal and measured emission trace, as illustrated in figure 5.11.

During our experimental campaign at JET, spectra for the singlet lines at 668 nm and 502 nm, and for the triplet lines at 588 nm, 389 nm, 707 nm, and 447 nm were taken. For 397 nm, 471 nm, and 728 nm the signals were too small to be analysed.

Two discharges, namely #49030 (L-mode) with 668 nm and #49504 (H-mode) with 588 nm are presented in this section. The T_e- profiles used for the model calculations (see figures 5.12 and 5.13) were taken from ECE measurements, the n_e profiles from JET ppf (processed pulse file) NFT2/PROF, i.e. a composition of LIDAR and infrared interferometry (KG1) data. Table 5.4 shows the He-beam parameters used for calculation of the line-emission profiles for the regarded discharges.

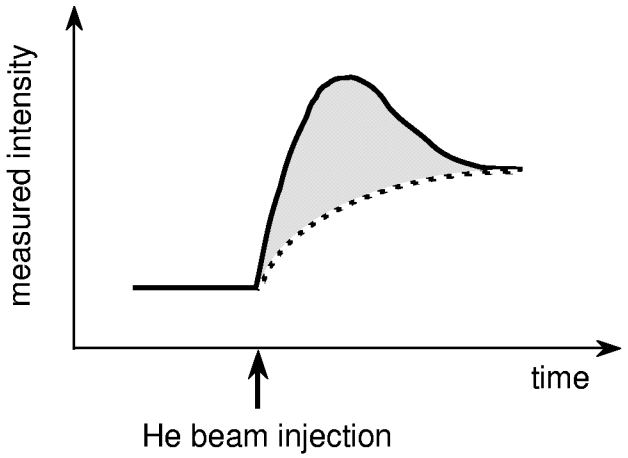

Figure 5.11: Illustration of the time-trace method for determination of the He-beam emission. The intensity of the signal emitted from the He beam (grey area) is obtained by subtracting the background signal (deduced from measurement of the pressure change in the injector, broken line) from the measured emission trace (solid line).

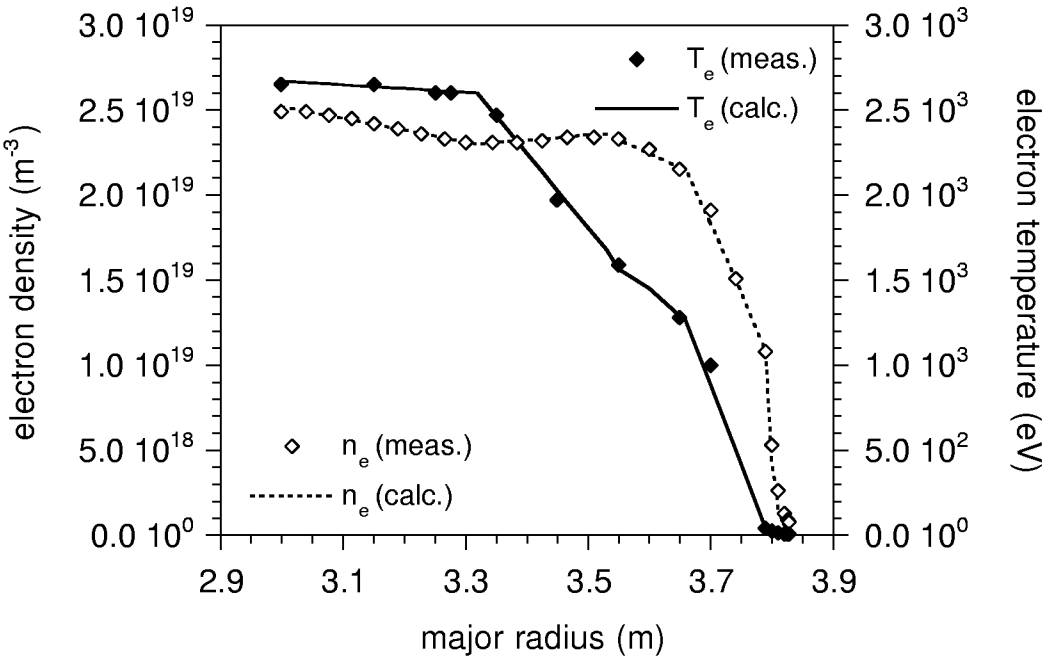

Figure 5.12: T_e and n_e profiles of JET discharge #49030: ECE-, LIDAR- and interferometry measurement results (diamonds) and therefore derived profiles which have been used for model calculations (lines).

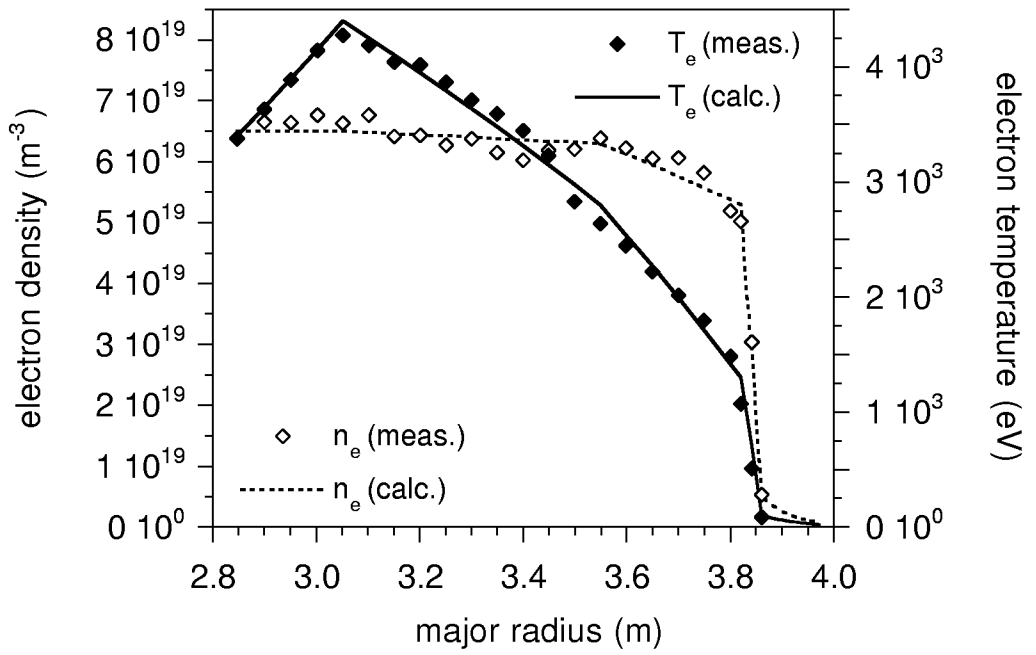

Figure 5.13: T_e and n_e profiles of JET discharge #49504: ECE-, LIDAR- and interferometry measurement results (diamonds) and therefore derived profiles which have been used for model calculations (lines).

discharge number	equivalent beam current	beam energy	measured wavelength	corresponding transition
49030	4 A	75 keV	668 nm	$3^1D \rightarrow 2^1P$
49504	4 A	80 keV	588 nm	$3^3D \rightarrow 2^3P$

Table 5.4: Discharge number, beam parameters and observed wavelength of the presented measurements at JET.

The spectra taken at JET show a higher ratio between shifted and unshifted intensity. In particular, the intensity of shifted triplet lines can exceed that of the unshifted line (see figure 5.10). The reason for this more favourable ratio is, on the one hand, the higher percentage of metastable atoms in the incident beam, since hydrogen gas instead of He is used for neutralization of the He-ion beam. On the other hand, the unshifted peak shows a lower intensity because the He-atom partial pressure in the plasma edge is lower than at AUG.

Due to the inclination of the beam against the radial direction (10° in horizontal- and 22.1° in vertical direction), the beam-path increment is not equal to the major-radius increment.

As already explained in section 5.1, a correction for the penetration depth compared to R_{maj} had to be applied. The values of R_{maj} and the corrected beam-path parameter L_{bi} at the separatrix and in the center of the plasma for the two presented discharges are given in table 5.5.

discharge number	R_{maj} at separatrix	L_{bi} at separatrix	R_{maj} at plasma center	L_{bi} at plasma center
49030	3.79 m	43 mm	3 m	1.004 m
49504	3.86 m	100 mm	3 m	0.710 m

Table 5.5: Major radius (R_{maj}) and beam-interaction length (L_{bi}) at the position of the separatrix and the plasma center for the two presented discharges.

Figures 5.14 to 5.15 show comparisons of measured and calculated line intensity profiles for these discharges, assuming an initial 2^3S fraction of 10%. As with the AUG experiments, the observed emission lines are well represented by the model calculations.

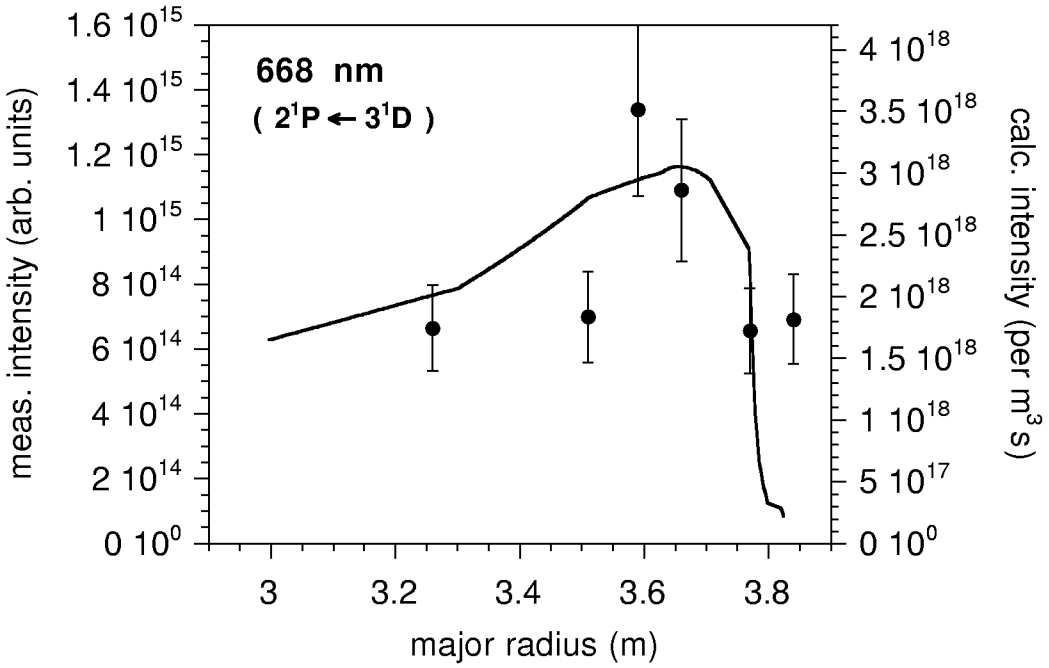

Figure 5.14: Comparison of the measured (circles) and calculated (solid line, assuming 10% 2^3S fraction) line emission at 668 nm for JET discharge #49030.

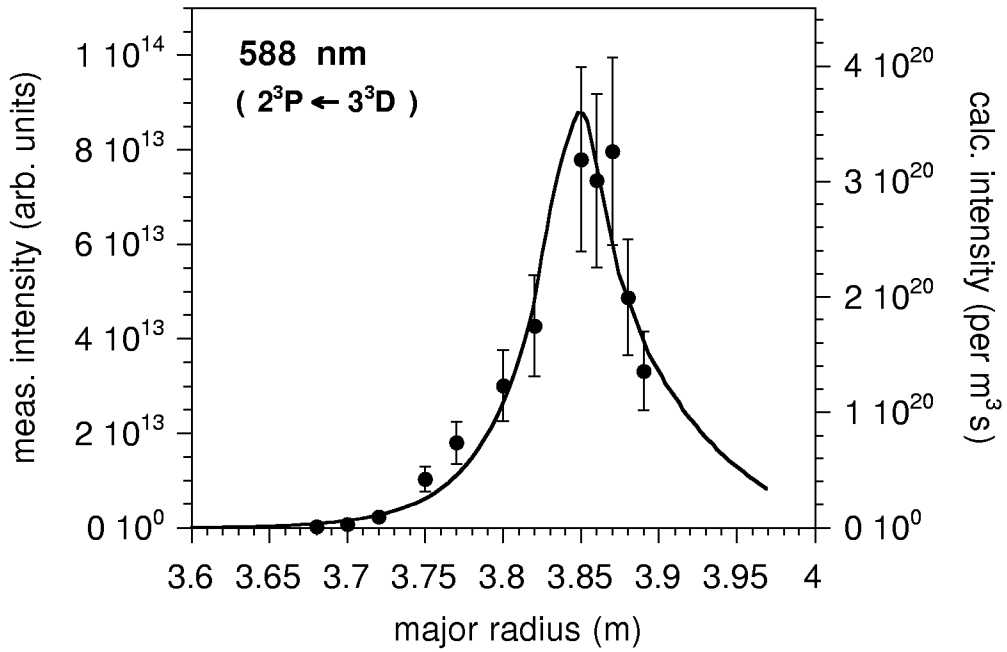

Figure 5.15: Comparison of the measured (circles) and calculated (solid line, assuming 10% 2^3S fraction) line emission at 588 nm for JET discharge #49504.

5.3 Conclusions from the Experiments

The concept of the pure He beam at AUG and the doped He beam at JET worked successfully, enabling for He beam-emission spectroscopy without major capital investment and without impeding the reliability and power of the neutral-beam heating systems. The intensities of the He-beam emission obtained from both He beams is sufficiently large to permit meaningful measurements for both HeI singlet- and triplet lines in the plasma. Comparison between measurement and model calculations show a favourable agreement. However, more effort is required to improve the mapping of the beam emission to the flux surfaces and to extend the evaluation to such measurements with better spatial resolution for the outer part of both AUG and JET plasmas.

During the second experimental phase at AUG - performed in May 2000 - also there a doped He beam has been used. For these measurements PINI 3 was utilized with the advantage of having a more favourable angle which allows for all lines of sight to separate the Doppler-shifted beam emission from the unshifted background emission. These experimental results are now being evaluated, but are not discussed in the course of this thesis.